Pergamon

Geochimica et Cosmochimica Acta, Vol. 66, No. 12, pp. 2287–2297, 2002

0016-7037/02 $22.00 + .00

PII S0016-7037(00)00824-9

Solubility behavior of alkali aluminosilicate components in aqueous fluids and silicate melts at high pressure and temperature

BJORN O. MYSEN[1,*†] and LORA ARMSTRONG[2]

[1]Geophysical Laboratory, Carnegie Institution of Washington, 5251 Broad Branch Road NW, Washington, DC, 20015-1305, USA
[2]Johns Hopkins University, Baltimore, MD, USA

(*Received April* 9, 2001; *accepted in revised form September* 18, 2001)

Abstract—The solubility behavior of K_2O, Na_2O, Al_2O_3, and SiO_2 in silicate-saturated aqueous fluid and coexisting H_2O-saturated silicate melts in the systems K_2O-Al_2O_3-SiO_2-H_2O and Na_2O-Al_2O_3-SiO_2-H_2O has been examined in the 1- to 2-GPa pressure range at 1100°C. Glasses of Na- and K-tetrasilicate compositions with 0, 3, and 6 mol% Al_2O_3 were used as starting materials. In both systems, the oxides dissolve incongruently in aqueous fluid and silicate melt. When recalculated to an anhydrous basis, the aqueous fluids are enriched in alkalis and depleted in silica and alumina relative to their proportions in the starting materials. The extent of incongruency is more pronounced in the Na_2O-Al_2O_3-SiO_2-H_2O system than in the K_2O-Al_2O_3-SiO_2-H_2O system.

The partition coefficients of the oxides, $D_{oxide}^{fluid/melt}$, are linear and positive functions of the oxide concentration in the fluid for each composition. There is a slight dependence of the partition coefficients on bulk composition. No effect of pressure could be discerned. For alkali metals, the fluid/melt partition coefficients range from 0.06 to 0.8. For Al_2O_3 this range is 0.01 to 0.2, and for SiO_2, it is 0.01 to 0.32. For all compositions, $D_{K_2O}^{fluid/melt} \sim D_{Na_2O}^{fluid/melt} > D_{SiO_2}^{fluid/melt} > D_{Al_2O_3}^{fluid/melt}$ for the same oxide concentration in the fluid. $D_{K_2O}^{fluid/melt}$, $D_{Na_2O}^{fluid/melt}$, and $D_{SiO_2}^{fluid/melt}$ correlate negatively with the Al_2O_3 content of the systems. This correlation is consistent with a solubility model of alkalis that involve associated KOH°, NaOH°, silicate, and aluminate complexes. *Copyright © 2002 Elsevier Science Ltd*

1. INTRODUCTION

Evidence for interaction between rocks and aqueous fluids in the crust and the upper mantle of the Earth is extensive. This evidence includes high-grade metamorphism in deep continental crust where dehydration of hydrous minerals has been associated with alteration of major and trace element contents (e.g., Rollinson and Windley, 1980; Fowler, 1984; Whitehouse, 1989). In metamorphic rocks near convergent plate boundaries, there is evidence for transport of major, minor, and trace elements from the subducting slab to the overlying mantle wedge (e.g., Brenan et al., 1995; McInnes, 1996; Riter and Smith, 1996). Contamination of source regions of magmatic liquids in island arcs by slab-derived fluids is also frequently suggested (e.g., Morris et al., 1990; Bebout et al., 1993; Plank and Langmuir, 1993).

To describe fluid–rock interaction processes in the upper mantle, experimental data on the solubility behavior of silicate components in aqueous fluids as a function of pressure, temperature, and bulk chemical composition is necessary. Some data exist. For example, the silicate solubility in aqueous fluids in the SiO_2-H_2O system is positively correlated with fluid density (Manning, 1994). Because fluid density is a positive function of pressure (e.g., Haar et al., 1984), silica solubility in aqueous fluid in the SiO_2-H_2O system increases with increasing pressure. In chemically more complex systems such as MgO-SiO_2-H_2O, it has been suggested that the solution behavior of silicate in aqueous fluids might depend on pressure (Fujii et al., 1996; Stalder et al., 2001). At pressures <3 GPa, the fluids contains only silica (Fujii et al., 1996; Zhang and Frantz, 2000), whereas at high pressure, MgO may become significantly soluble (Fujii et al., 1996; Stalder et al., 2001). Pressure-dependent solubility behavior of major elements in aqueous fluid has also been reported in the $NaAlSi_3O_8$-H_2O system (Stalder et al., 2000).

Temperature also affects the solubility behavior of major elements in aqueous fluids. The silicate solubility in aqueous fluids increases and the H_2O solubility in coexisting silicate melts sometimes increases with increasing temperature resulting in shrinkage of the silicate-H_2O solvus (Kennedy et al., 1962; Paillat et al., 1992; Manning, 1994). There may be complete miscibility between aqueous fluids and at least some alkali aluminosilicate melts in the pressure–temperature regime of the upper mantle (Shen and Keppler, 1997; Bureau and Keppler, 1999).

The solubility of H_2O of individual oxide components such as SiO_2 and Al_2O_3 can be quite different (e.g., Anderson and Burnham, 1967; Pascal and Anderson, 1989). In multicomponent silicate systems, one might, therefore, expect that the solution behavior in aqueous fluids is incongruent. Such behavior has been observed for $NaAlSi_3O_8$-H_2O, for example (Anderson and Burnham, 1967; Stalder et al., 2000).

Partition coefficients of alkalis, alumina, and silica between coexisting aluminosilicate melts and aqueous fluids most likely depend, therefore, on pressure and temperature as well as bulk chemical composition. However, experimental data relevant to such relationships remain relatively uncommon, in particular in multicomponent systems relevant to rock-forming processes in

* Author to whom correspondence should be addressed (mysen@gl.ciw.edu).
† B.O.M. is a member of the NSF-sponsored Center for High-Pressure Research.

Table 1. Composition of starting materials (wt%).[a]

Element	KS4	KS4A3	KS4A6
SiO_2	72.27 (1.20)	71.22 (0.84)	72.73 (0.64)
Al_2O_3	0.11 (0.06)	4.87 (0.15)	8.63 (0.12)
K_2O	27.47 (0.27)	23.84 (0.21)	18.93 (0.25)

[a] Average of 10 individual analyses.

the Earth's lower crust and upper mantle. An experimental study was carried out in the system K_2O-Na_2O-Al_2O_3-SiO_2-H_2O in the 1.0- to 2.0-GPa pressure range at 1100°C to provide such data.

2. EXPERIMENTAL METHODS

Starting compositions were in the systems K_2O-Al_2O_3-SiO_2-H_2O and Na_2O-Al_2O_3-SiO_2-H_2O. In both systems, the Al-free end members were K- and Na-tetrasilicate (denoted KS4 and NS4, respectively). The degree of polymerization (NBO/Si) of molten KS4 and NS4 corresponds to that typically observed for andesite melt (e.g., Mysen, 1987). Three and 6 mol% Al_2O_3 were added in charged-balanced form ($Na^+ = Al^{3+}$ and $K^+ = Al^{3+}$, respectively) to these compositions (denoted KS4A3, KS4A6, NS4A3, and NS4A6 for K- and Na-aluminosilicate compositions, respectively). Under the assumption that this Al^{3+} is tetrahedrally coordinated in the melts of these compositions, their NBO/T (T = Al + Si) decreases as the alumina content is increased (to 0.32 with 3 mol% Al_2O_3 and 0.17 with 6 mol% Al_2O_3). This range in NBO/T corresponds to that typically found in molten dacite and rhyolite (Mysen, 1987). The solubility data may therefore be employed to characterize the distribution of alkalis, alumina, and silica between magmatic liquids and aqueous fluid.

The anhydrous silicate starting materials were glasses formed by mixing K_2CO_3 + Al_2O_3 + SiO_2 and Na_2CO_3 + Al_2O_3 + SiO_2, respectively, under alcohol for ~1 h, decarbonated by slow heating (~1°C/m), and finally melted at temperatures ~100°C above the individual liquidii (liquidus phase relations from compilations by Osborn and Muan, 1960a,b) in $MoSi_2$-heated 1-atm furnaces. The glasses formed upon quenching (Table 1) were crushed to ~20-μm grain size and stored at 110°C when not used.

High-pressure experiments were conducted in the solid-media, high-pressure apparatus (Boyd and England, 1960) with 3/4-inch-diameter tapered furnace assemblies (Kushiro, 1976). Pressure was calibrated with the calcite–aragonite and quartz–coesite transitions and the melting point of NaCl. Precision is <0.05 GPa and accuracy ≤0.1 GPa. Temperature was measured with Pt-$Pt_{90}Rh_{10}$ thermocouples with no pressure correction on the electromotonic force (emf) of the thermocouples. Temperature precision is ±1°C. Temperature accuracy is ≤10°C.

The high-pressure experiments were conducted with a double-capsule technique slightly modified after Schneider and Eggler (1986). The anhydrous glass starting material (10- to 40-mg glass sample) was loaded into 3-mm outer diameter (2.6-mm inner diameter) and 5- to 6-mm-long Pt capsules perforated with 200-μm holes (~50 randomly distributed holes) and sealed on both ends (Schneider and Eggler 1986 used an inner capsule crimped, but not sealed, on both ends). This capsule was loaded into an outer 5-mm outer diameter Pt capsule together with the desired amount of H_2O and welded shut; 1- to 50-μL double-distilled and deionized H_2O was loaded with a microsyringe. Weighing errors introduced with this method were ≤1%. The holes in the inner capsule served as pathways for the aqueous fluid initially in the outer capsule to communicate with the silicate melt in the inner capsule (experiments at 1100°C were above the temperatures of the H_2O-saturated liquidus for the compositions used). In this design, the inner capsule collapsed on the sample at high pressure so that the amount of excess fluid over that dissolved in the melt in the inner capsule was essentially zero. Therefore, after temperature quenching of an experiment, H_2O-saturated silicate melt in the inner capsule and quenched fluid (with abundant quench precipitates) in the outer capsule were physically separated. After an experiment, the inner capsule was removed and physically cleaned under a 50× magnification binocular microscope, then cleaned with distilled H_2O in an ultrasonic cleaner to remove all materials from the outer capsule wall. The H_2O-saturated glass in the inner capsule was then removed.

The quenched glass was analyzed with a JEOL 8900 electron microprobe operating at 15 kV and 10 nAmp current with a 10 × 10μm rastered square and 30-s integration time. Before it was subjected to analysis, the silicate glass was diluted with $LiBO_2$ ($LiBO_2$:silicate = 5:1) and remelted at 950°C for 1 h at ambient pressure. This dilution with $LiBO_2$ was necessary to avoid alkali volatilization under the electron beam. In undiluted form, the most volatile glasses, NS4 and KS4, exhibited ~20% loss of Na_2O and K_2O after 30 s under the electron beam. No loss could be detected in the $LiBO_2$-diluted samples with the same integration time. Ten or more points were analyzed for each sample. The quoted errors are the standard error of the average of the individual data points.

Because of extensive precipitation of silicate from the silicate-saturated fluid during quenching, fluid extracted from the outer capsule does not represent the equilibrium composition (see Mysen and Wheeler, 2000a, for detailed documentation). The fluid composition was, therefore, calculated by mass-balance by using the analyzed starting glass composition and the analyzed composition of the quenched glass. In this calculation, the proportion of coexisting H_2O-saturated silicate melt and silicate-saturated aqueous fluid in an experiment was derived from the measured proportion of glass and H_2O in the starting materials and the H_2O and silicate solubilities in melt and fluid, respectively, at the pressure and temperature of each experiment (solubility data from Mysen and Acton, 1999, and Mysen and Wheeler, 2000a,b). The actual weight fraction of aqueous fluid in an experiment, X_f, is therefore related to the weight fraction of fluid in the starting composition, X_{H_2O}, as follows:

$$X_f = \frac{\left(\frac{X_{H_2O}}{1 - X_{H_2O}}\right)\left(\frac{1 - X_{H_2O}^{melt}}{1 - X_{silicate}^{fluid}}\right)}{1 + \left(\frac{X_{H_2O}}{1 - X_{H_2O}}\right)\left(\frac{1 - X_{H_2O}^{melt}}{1 - X_{silicate}^{fluid}}\right)}, \quad (1)$$

where $X_{H_2O}^{melt}$ and $X_{silicate}^{fluid}$ are the solubilities of H_2O in melt and of silicate in coexisting aqueous fluid as weight fractions. The reported uncertainties of oxide concentrations in the aqueous fluid incorporate the errors introduced in each of the analytical and computational steps. The uncertainties in the solubilities, $X_{H_2O}^{melt}$ and $X_{silicate}^{fluid}$, used in this calculation are those reported by Mysen and Acton (1999) and Mysen and Wheeler (2000a,b).

Attainment of equilibrium was addressed with time studies. At 1100°C, experimental durations between 800 and 1440 min were needed to reach fluid/melt partition coefficients that were independent of experimental duration (Fig. 1). This experimental duration is also consistent with H_2O diffusion control of equilibration. The maximum H_2O transport distance in the melt in the inside Pt capsule is ~1.3 mm. From the simple relationship, $x = (4Dt)^{1/2}$ (x = travel distance, D = diffusion constant, and t = time), this transport distance (1.3 mm) at 1440 min requires a diffusion coefficient for H_2O in the melts of $\sim 4 \times 10^{-8}$ cm^2/s. This value is near the upper end of the range of diffusion coefficients reported for H_2O in melts of basaltic to rhyolitic composition (10^{-6} to 10^{-8} cm^2/s in the same temperature range; see Zhang et al., 1991; Nowak and Behrens, 1997). All experiments were therefore conducted with experimental durations ≥1440 min.

3. RESULTS AND DISCUSSION

3.1. Solubility Behavior

A summary of compositions of coexisting melts and fluids, recalculated to anhydrous silicate compositions, in the systems K_2O-Al_2O_3-SiO_2-H_2O (KAS) and Na_2O-Al_2O_3-SiO_2-H_2O (NAS), is shown in Figure 2 (analytical data are available from the authors on request). The aqueous fluid is enriched in alkalis (K_2O and Na_2O) relative to the coexisting melts. In the KAS system (Fig. 2A), aqueous fluids also show Al_2O_3 depletion, and the melts show Al_2O_3 enrichment. This latter trend is more

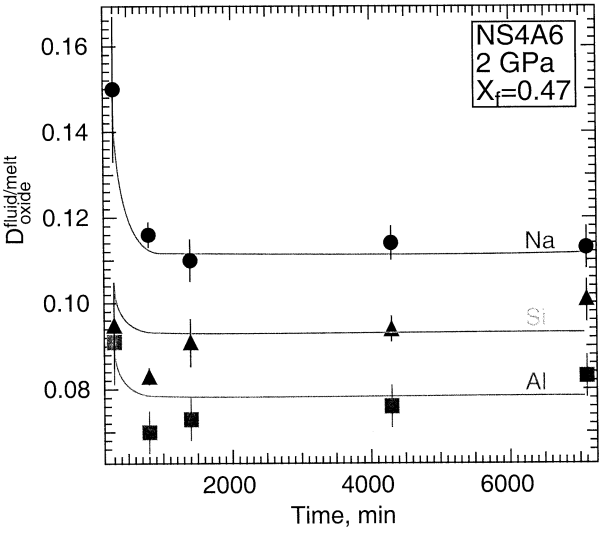

Fig. 1. Fluid/melt partition coefficients, $D^{fluid/melt}_{oxide}$, as a function of experimental duration (time) for composition NS4A6 at 2 GPa and fluid fraction $X_f = 0.47$.

subtle in the NAS system (Fig. 2B). It is therefore clear that in these two alkali aluminosilicate systems, solution in the aqueous fluids is distinctly incongruent. As a result, the composition of coexisting melts is also nonstoichiometric. This effect is observed in both systems, but the compositional difference between coexisting fluids and melts is more pronounced in the K-aluminosilicate system than in the Na-aluminosilicate system.

Incongruent solubility behavior of alkali aluminosilicate components in fluids has also been observed in other systems such as $NaAlSi_3O_8$-H_2O in the 0.5- to 1.5-GPa and 630 to 775°C pressure and temperature range (Stalder et al., 2000) and in aqueous fluid coexisting with Spruce Pine pegmatite in the 0.3- to 1.0-GPa and 500 to 650°C pressure and temperature range (Burnham, 1967). A difference between those latter data and the results summarized in Figure 2 is that in the latter data set the aqueous fluids were distinctly enriched in SiO_2 component compared with the condensed silicate (whether crystalline or molten), whereas in the present results, the alkali/silica ratio (whether K or Na) of the aqueous fluids is higher than in the coexisting melt. However, there are several important differences between the data in Figure 2 and those reported by Burnham (1967) and Stalder et al. (2000). In the latter two experimental studies, the alumina contents were considerably higher, with their alkali/alumina ratio near unity (the systems are nearly meta-aluminous). In contrast, in the present experiments, the systems were peralkaline (alkali/alumina > 1) and the temperature was considerably higher (1100°C compared with <750°C in the database of Burnham 1967 and Stalder et al. 2000). Temperature not only affects the bulk solute content (e.g., Pascal and Anderson, 1989; Manning, 1994; Mysen and Acton, 1999; Stalder et al., 2000; Zhang and Frantz, 2000), it also most likely affects the solubility mechanism of silicate in aqueous fluids (Stalder et al., 2000; Zhang and Frantz, 2000). For example, in aqueous fluid coexisting with $NaAlSi_3O_8$ (albite) at 1.7 GPa, the SiO_2 in the fluid is higher than that of $NaAlSi_3O_8$ at 625 to 650°C, whereas at higher temperature and

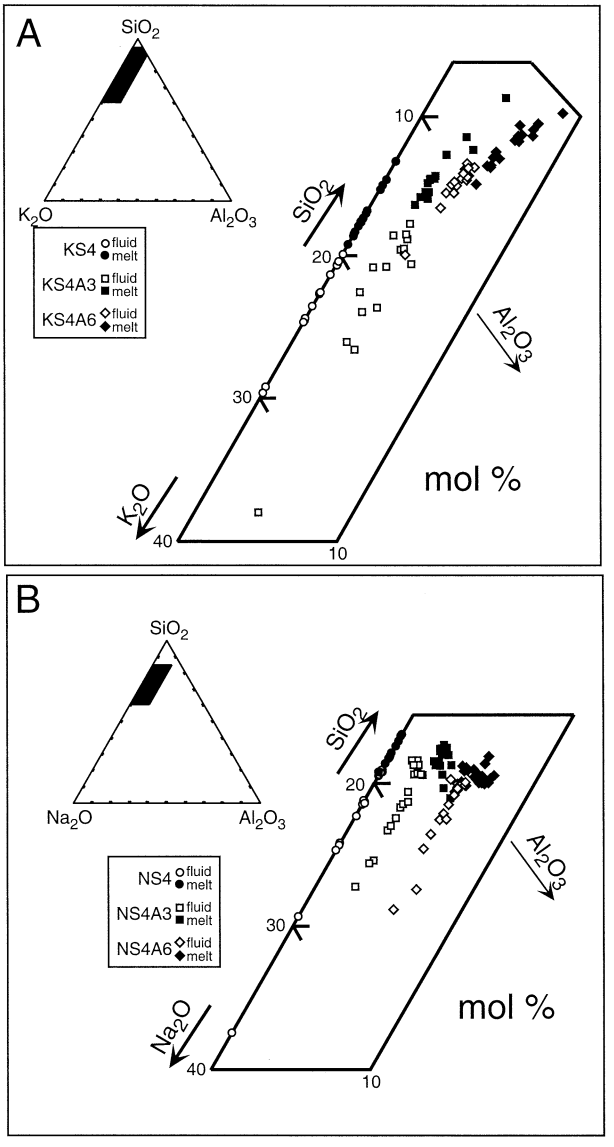

Fig. 2. Bulk composition of silicate-saturated aqueous fluid and coexisting H_2O-saturated silicate melts recalculated on an anhydrous basis (A) K_2O-Al_2O_3-SiO_2-H_2O and (B) Na_2O-Al_2O_3-SiO_2-H_2O. Open symbols, silicate-saturated aqueous fluid; solid symbols, H_2O-saturated silicate melt.

the same pressure, the SiO_2 content of the fluid is less than that of $NaAlSi_3O_8$ (Stalder et al., 2000).

In a meta-aluminous alkali aluminosilicate system such as $NaAlSi_3O_8$, alkali-charge-balanced aluminate complexes may be the dominant species in the aqueous fluid. This suggestion is consistent with a positive correlation between Al_2O_3 solubility and KOH content of aqueous fluids (e.g., Pascal and Anderson, 1989). In comparison, in the present experiments the alkali/alumina > 1 so that excess alkali over that required to stabilize aluminate complexes may dissolve in aqueous fluids, perhaps as simple hydrolyzed alkali complexes and possibly as alkali silicate complexes (Mysen, 1998). Such solute complexes are likely to be associated because the dielectric constant of H_2O decreases rapidly with increasing temperature (e.g., Pitzer,

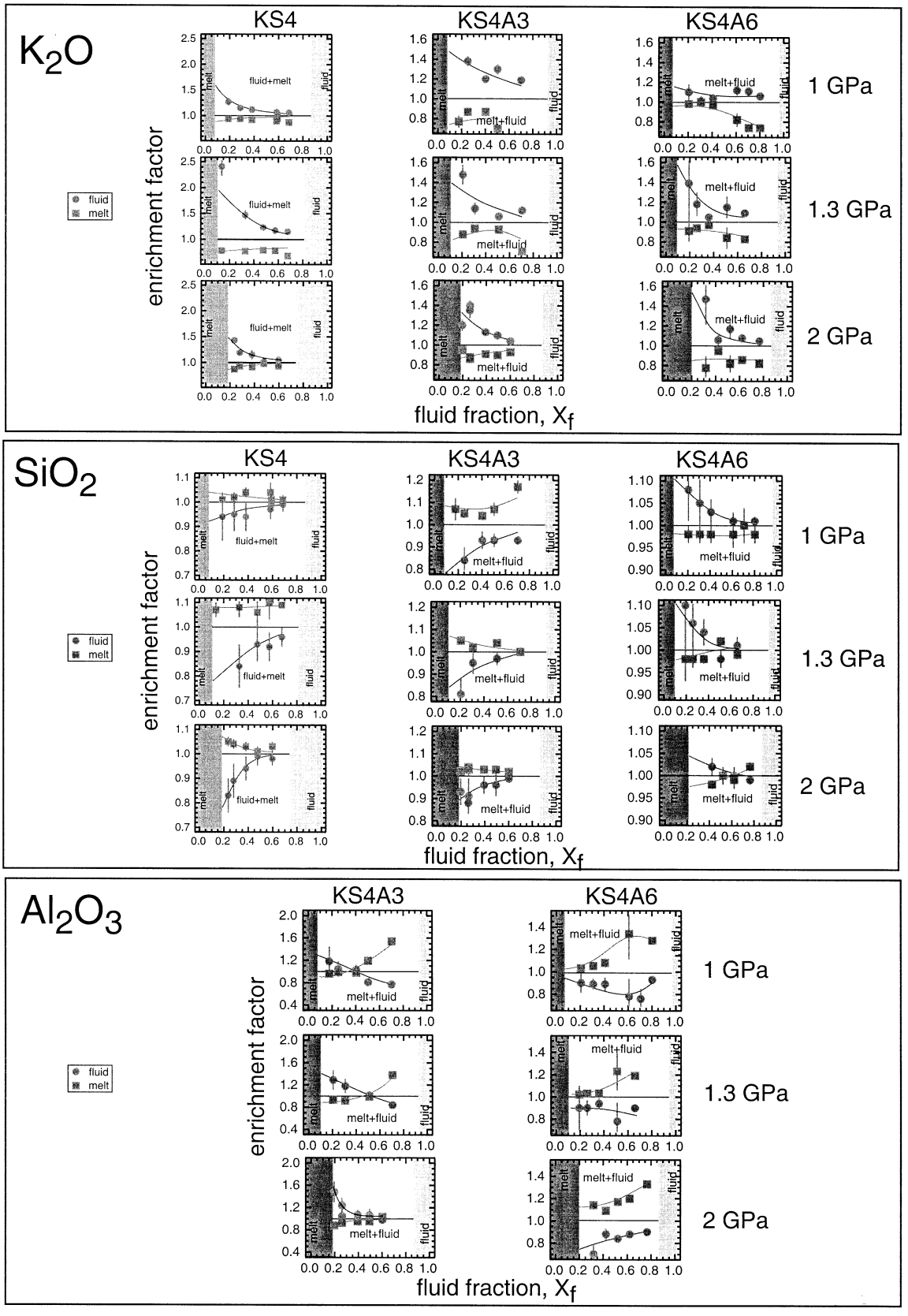

Fig. 3. Enrichment factors calculated as shown in Eqn. 2 for silicate-saturated aqueous fluid (circles) and coexisting H_2O-saturated silicate melts (squares) as a function of fluid fraction, X_f, and pressure in the system K_2O-Al_2O_3-SiO_2-H_2O. The fields marked "melt," "melt + fluid," and "fluid" are delineated after Mysen and Acton (1999).

1983). Decreasing dielectric constant promotes association of the solute. In analogy with other salt solutes in aqueous fluids (e.g., Quist and Marshall, 1968; Frantz and Popp, 1981), association constants of alkali-OH complexes are likely to increase with increasing temperature.

For the same reason, associated alkali silicate complexes in the aqueous fluids likely become increasingly abundant the higher the temperature. It is suggested that these differences (temperature and bulk composition) account for the different solution behavior observed by Burnham (1967) and Stalder et al. (2000) compared with the data from the present systems.

Details of the compositional evolution of coexisting silicate-saturated aqueous fluid and H_2O-saturated silicate melts as a function of fluid fraction, X_f, and pressure are shown in Figures 3 and 4. The enrichment factor, EF, used in Figures 3 and 4 is defined as follows:

$$EF = \text{oxide (m,f)/oxide(starting material).}$$

The values of oxide(m,f) are the oxide concentrations (wt%) of melts, oxide(m), and aqueous fluid, oxide(f), recalculated to an H_2O-free basis. The recalculation to anhydrous silicate compositions of fluids and melts was carried out with the aid of the solubility data from Mysen and Acton (1999) and Mysen and Wheeler (2000a,b).

Also shown in Figures 3 and 4 as shaded regions are the fields where only H_2O-bearing melt ("melt") and silicate-bearing fluid ("fluid") are stable (Mysen and Acton, 1999; Mysen and Wheeler, 2000a,b). The boundary between "melt" and "fluid + melt" represents the H_2O solubility in the melt and the boundary between "fluid + melt" and "fluid" the bulk silicate solubility on the aqueous fluid.

Alkali enrichment factors in aqueous fluids above 1 are evident for all compositions and at all pressures (Figs. 3 and 4). As the fraction of fluid, X_f, decreases toward the "melt"/"melt + fluid" boundary, the alkali enrichment in the fluid increases. The alkalis in the coexisting melt show a concomitant decrease. For Al-free Na-tetrasilicate, the enrichment factor near the "melt"/"melt + fluid" boundary decreases with increasing pressure (Fig. 4). For the equivalent K-tetrasilicate composition (Fig. 3), the data near this boundary are less precise but consistent with a similar trend. In the Al-bearing systems (NS4A3, NS3A6, KS4A3, KS4A6) no such pressure effect can be discerned. We suggest, therefore, that the extent of incongruency (difference between melt and fluid composition) diminishes with increasing pressure.

The solubility behavior of silica is somewhat more complex. For the Al-free compositions (KS4 and NS4), the enrichment factor for SiO_2 in aqueous fluid decreases and that of the melt increases as the fluid fraction, X_f, decreases. As for alkalis, the effect of melt/fluid ratio on the silica enrichment factors decreases with increasing pressure for the NS4 composition, whereas the less detailed data for KS4 composition can only be considered consistent with such a trend. With 3 mol% Al_2O_3, both systems show the same silica trends (with the exception of NS4A3 at 1 GPa, where there is a very small effect of X_f). This feature remains at 6 mol% Al_2O_3 in the Na_2O-Al_2O_3-SiO_2-H_2O system (Fig. 4), whereas in the K_2O-Al_2O_3-SiO_2-H_2O system, the SiO_2 enrichment factor remains above 1 as the fluid fraction in the system, X_f, is reduced (Fig. 3).

The behavior of Al_2O_3 in these systems is complicated by the presence of trace amounts of corundum coexisting with fluids and melts in fluid-rich ($X_f > 0.6$) portions of both the KS4A6 and NS4A6 systems (Mysen and Acton, 1999; Mysen and Wheeler, 2000a). Although corundum was not reported in experimental charges from either KS4A3 or NS4A3, trace amounts could have been overlooked. Although the proportion of corundum could not be quantified in those studies (but most likely less than 1% of the mode), mass-balance calculation of Al_2O_3 in the fluid based on an assumption that all Al_2O_3 in the system resided in silicate melt and aqueous fluid will be inaccurate. Thus, the enrichment factors in the high-X_f portion of those systems will also be in error although the magnitude of this error cannot be estimated. For compositions near the "melt"/"melt + fluid" boundaries, there was no evidence for corundum, and the enrichment factors reported for Al_2O_3 are more reliable. Interestingly, near this boundary, the enrichment factors generally do not differ greatly from 1 (Figs. 3 and 4).

3.2. Fluid/Melt Partitioning

The partition coefficients, $D_{K_2O}^{fluid/melt}$ and $D_{Na_2O}^{fluid/melt}$,[1] at the "melt"/"melt + fluid" boundary are higher than at higher X_f values regardless of pressure (Figs. 3 to 5). $D_{K_2O}^{fluid/melt}$ and $D_{Na_2O}^{fluid/melt}$ are negatively correlated with Al_2O_3 of the system and approach the values for $D_{Al_2O_3}^{fluid/melt}$ for the most aluminous compositions. This evolution probably reflects changes in solution mechanism of sodium and potassium in the fluid (and melt) as Al_2O_3 is added. That suggestion is supported by the observation of Pascal and Anderson (1989), who found that Al_2O_3 solubility in aqueous solution at several hundred MPa pressure is linearly and positively correlated with KOH concentration in aqueous fluid. These relationships may exist because alkali metals may in part serve to charge-balance Al^{3+} in aluminate complexes in the fluid in analogy with the solution behavior of Al^{3+} in silicate melts (see, e.g., Mysen, 1995, for review of information) and in part as hydrolyzed alkli-OH complexes. Such a solubility mechanism may explain why $D_{K_2O}^{fluid/melt}$ and $D_{Na_2O}^{fluid/melt}$ decrease with increasing Al_2O_3 content.

$D_{SiO_2}^{fluid/melt}$ is also negatively correlated with Al_2O_3 (Fig. 5). This behavior may be rationalized by considering possible silicate and aluminate complexes in the aqueous fluids. Zhang and Frantz (2000) suggested from their solubility experiments in the system MgO-SiO_2 that silicate species in aqueous fluids in the pressure/temperature regime under discussion may occur as various depolymerized silicate species.[2] This suggestion is supported by results from recent in situ, high-temperature, and high-pressure Raman spectroscopy of aqueous fluids in equilibrium with $K_2Si_4O_9$ melt and with crystalline SiO_2 (Mysen, 1998; Zotov and Keppler, 2000). Some of these silicate complexes may be associated with alkali metals in excess of that

[1] The partition coefficient is defined as $D^{fluid/melt} = oxide^{fluid}/oxide^{melt}$ (mol%). Note that whereas the enrichment factor, EF, used in Figures 3 and 4 is calculated on an anhydrous basis for both fluids and melts, the partition coefficient, $D^{fluid/melt}$, in Figures 5 to 7, is calculated with the actual oxide concentrations in silicate-saturated aqueous fluid and H_2O-saturated silicate melt.

[2] A depolymerized silicate complex is one where the silicate tetrahedra contain nonbridging oxygen.

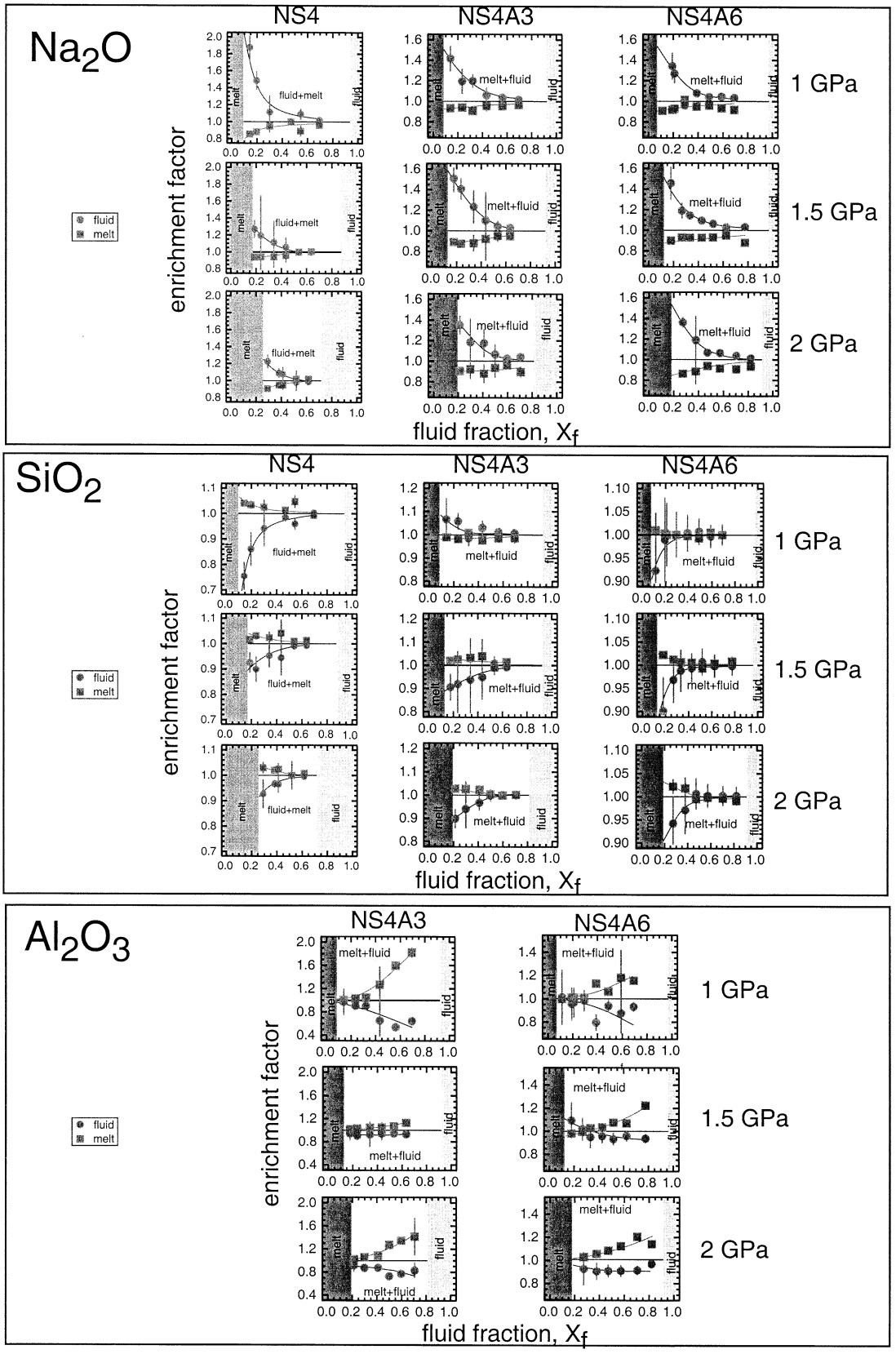

Fig. 4. Enrichment factors calculated as shown in eqn (2) for silicate-saturated aqueous fluid (circles) and coexisting H_2O-saturated silicate melts (squares) as a function of fluid fraction, X_f, and pressure in the system Na_2O-Al_2O_3-SiO_2-H_2O. The fields marked "melt", "melt+fluid", and "fluid" delineated after Mysen and Wheeler (2000a, b).

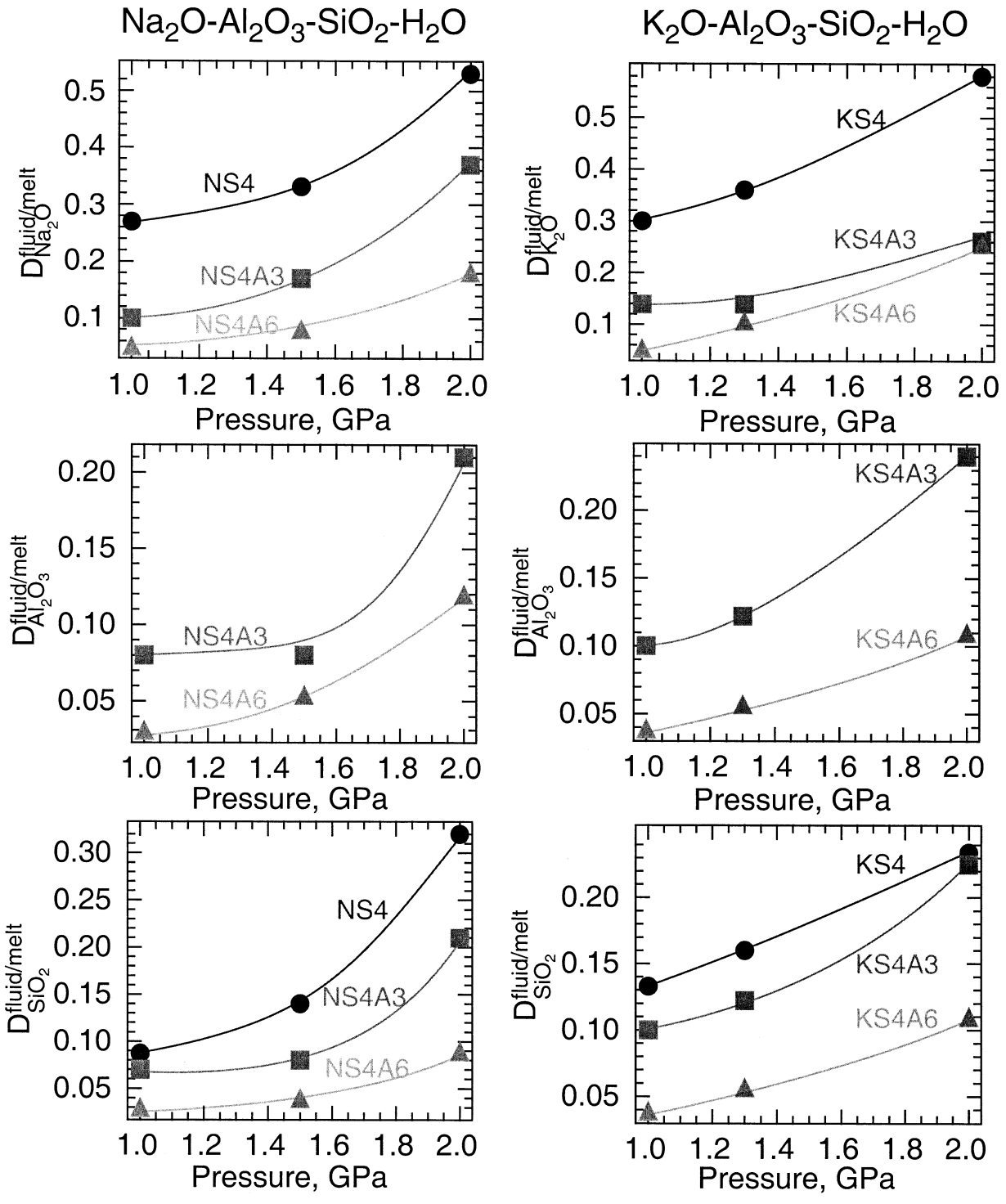

Fig. 5. Fluid/melt partition coefficients, $D^{fluid/melt}_{Na_2O}$, $D^{fluid/melt}_{Al_2O_3}$, $D^{fluid/melt}_{SiO_2}$, and $D^{fluid/melt}_{K_2O}$, at the boundary between "fluid + melt" and "melt" (see Figs. 3 and 4) as a function of pressure for compositions indicated. Lines connecting the points are simply meant to guide the eye.

required to stabilize tetrahedrally coordinated Al^{3+} in aluminate complexes. This suggestion stems from the observation (Mysen, 1998) that at least for aqueous fluids in the system $K_2Si_4O_9$-H_2O at pressures and temperatures approximately the same as in the present experiments, isolated SiO_4^{4-} complexes are protonated (i.e., H_4SiO_4). For the more polymerized silicate complexes that also exist in these fluids, K^+, but not H^+, serves to neutralize nonbridging oxygen in the silicate complex. Mysen (1998), by using in situ, high-temperature, high-pressure Raman spectroscopy in a diamond anvil cell, concluded

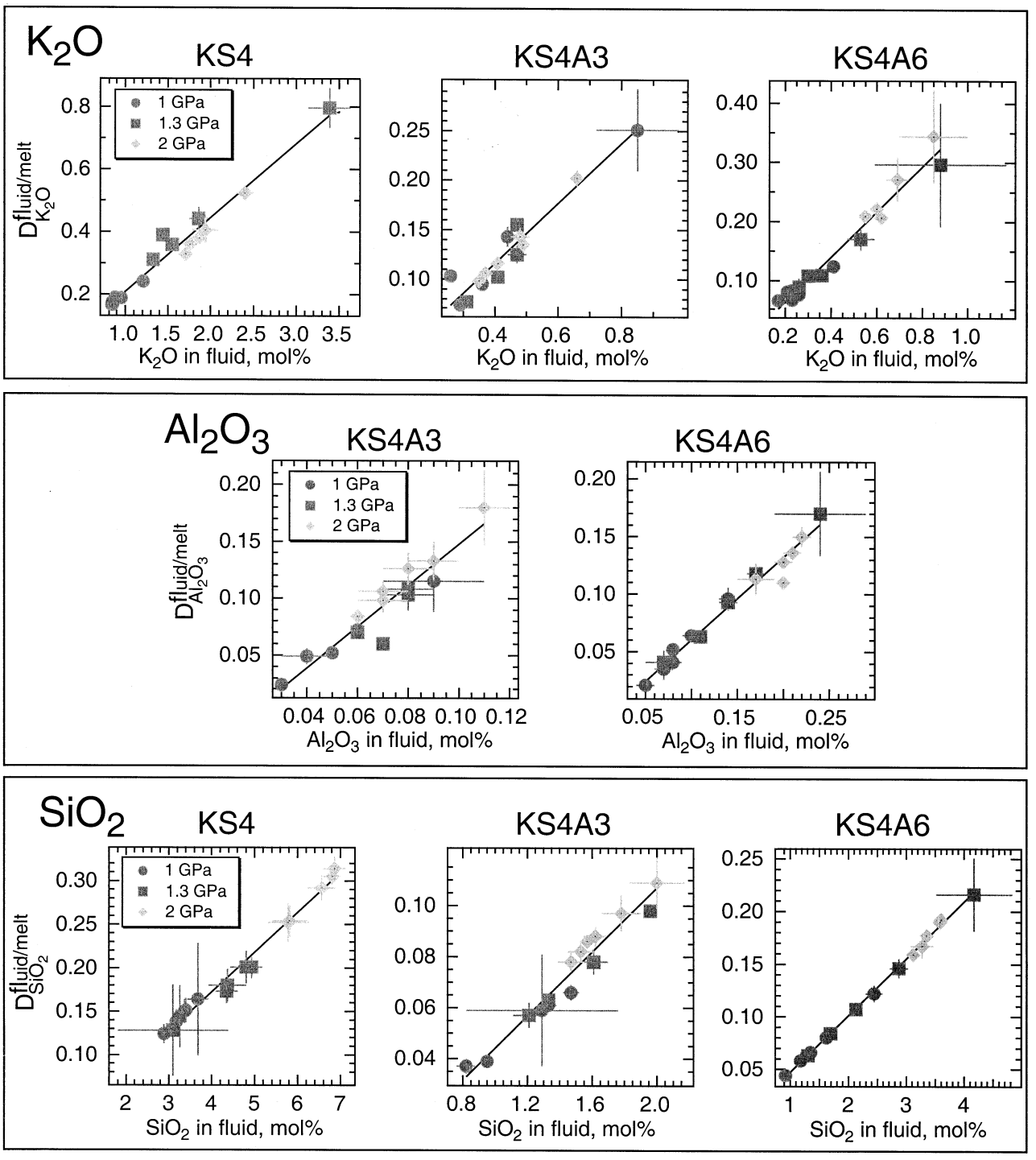

Fig. 6. Fluid/melt partition coefficients, $D^{fluid/melt}_{K_2O}$, $D^{fluid/melt}_{Al_2O_3}$, and $D^{fluid/melt}_{SiO_2}$, in the system K_2O-Al_2O_3-SiO_2-H_2O as a function of oxide concentration in aqueous fluid. Regression coefficients for the fits are given in Table 2.

that the principal complexes in the aqueous fluids in the $K_2Si_4O_9$-H_2O system resembled $H_4SiO^0_4$, $K_2SiO^0_3$, and $K_2Si_2O^0_5$. Association is likely at these high temperatures because the dielectric constant for H_2O is quite low (e.g., Pitzer, 1983). We suggest that excess alkalis over that needed for charge balance of Al^{3+} in aluminate complexes in the present systems may be similar to those observed by Mysen (1998) with both K^+ and Na^+ associated with aluminate and depolymerized silicate complexes. The larger the concentration of alumina, the less alkali is available for complexing with silicate species in the fluid (alkali activity is decreasing). As a result, the proportion of silica that can dissolve in the fluid

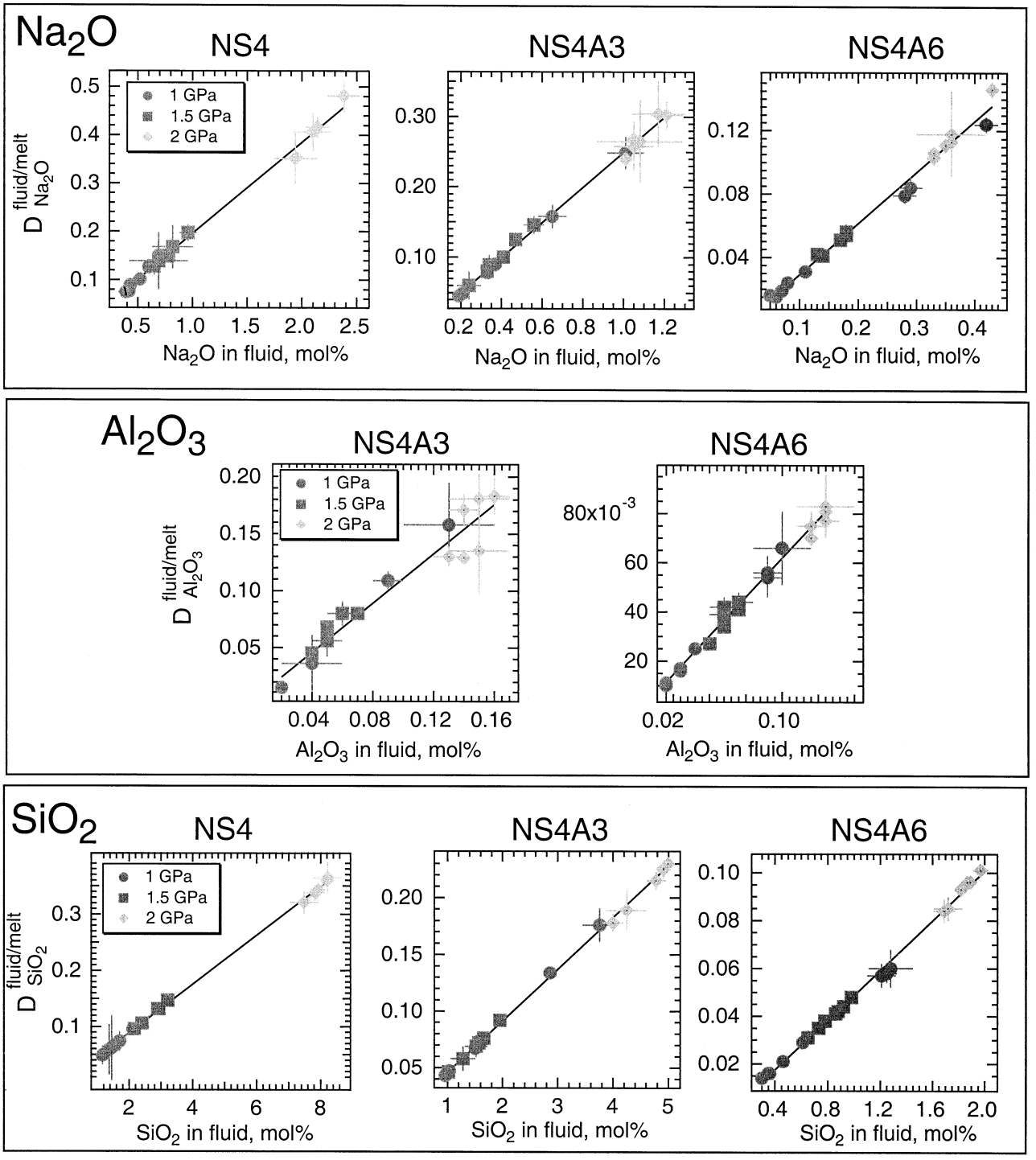

Fig. 7. Fluid/melt partition coefficients, $D^{fluid/melt}_{Na_2O}$, $D^{fluid/melt}_{Al_2O_3}$, and $D^{fluid/melt}_{SiO_2}$, in the system Na_2O-Al_2O_3-SiO_2-H_2O as a function of oxide concentration in aqueous fluid. Regression coefficients for the fits are given in Table 2.

would decrease with increasing Al_2O_3 content and so would $D^{fluid/melt}_{SiO_2}$. This behavior is exactly what is observed (Fig. 5).

For each composition, the partition coefficients $D^{fluid/melt}_{K_2O}$, $D^{fluid/melt}_{Na_2O}$, $D^{fluid/melt}_{Al_2O_3}$, and $D^{fluid/melt}_{SiO_2}$ are linear functions of the concentrations of individual oxide in the aqueous fluid (Figs. 6 and 7; Table 2). The oxide concentration in the fluid is governed by the fluid fraction, X_f, and pressure. These observations are consistent with a conclusion that in the relatively low concentration range of the oxides in the fluids, the solution behavior is Henrian.

$D^{fluid/melt}_{K_2O}$ and $D^{fluid/melt}_{Na_2O}$ are nearly identical at given oxide (K_2O or Na_2O) concentration and Al_2O_3. There is, however, a

Table 2. Regression coefficients for the expression $D^{fluid/melt}_{oxide} = a + b \times oxide_{fluid}$ (mol%)

$Oxide_{fluid}$	a	b	R^2
$K_2O \cdot Al_2O_3 \cdot SiO_2 \cdot H_2O$			
KS4			
K_2O	−0.03 (0.02)	0.236 (0.012)	0.96
Al_2O_3	—	—	—
SiO_2	−0.011 (0.007)	0.046 (0.001)	0.99
KS4A3			
K_2O	−0.005 (0.011)	0.303 (0.024)	0.93
Al_2O_3	−0.34 (0.012)	1.82 (0.17)	0.90
SiO_2	−0.018 (0.006)	0.063 (0.004)	0.95
KS4A6			
K_2O	−0.013 (0.010)	0.381 (0.020)	0.96
Al_2O_3	−0.012 (0.005)	0.718 (0.033)	0.97
SiO_2	−0.007 (0.002)	0.054 (0.006)	1.00
$Na_2O \cdot Al_2O_3 \cdot SiO_2 \cdot H_2O$			
NS4			
Na_2O	0.006 (0.005)	0.189 (0.004)	0.99
Al_2O_3	—	—	—
SiO_2	0.002 (0.002)	0.0434 (0.003)	1.00
NS4A3			
Na_2O	0.001 (0.003)	0.251 (0.004)	1.00
Al_2O_3	0.002 (0.003)	1.083 (0.068)	0.94
SiO_2	0.0002 (0.0013)	0.0456 (0.0003)	1.00
NS4A6			
Na_2O	0.003 (0.002)	0.323 (0.008)	0.99
Al_2O_3	−0.001 (0.001)	0.633 (0.016)	0.99
SiO_2	−0.0032 (0.0008)	0.0519 (0.0007)	1.00

slight effect of bulk composition on the linear relationships with oxide concentration in fluid. The fluid/melt partition coefficients become more sensitive to oxide concentration in the fluid as the systems become more aluminous (Figs. 6 and 7; Table 2). These relationships may be due to the proposed multiple structural roles of alkalis in aluminosilicate-saturated aqueous fluids (alkali hydrolysis and aluminate complexing; see above). To explain the composition dependence of $D^{fluid/melt}_{alkali}$ via the proposed solution mechanisms, $D^{fluid/melt}_{alkali}$ must exhibit different functional relationship to alkali content in the aqueous fluid, depending on whether alkalis are dissolved via simple hydrolysis or alkalis are dissolved in the form of aluminate complexes. Furthermore, if we assume that the KOH^0 and $NaOH^0$ (hydrolysis) and aluminate complexes in the fluids are similar in all fluid compositions, $D^{fluid/melt}_{alkali}$ for one of the Al-bearing compositions can be estimated from $D^{fluid/melt}_{alkali}$ values from the other Al-bearing and Al-free compositions. For example, $D^{fluid/melt}_{alkali}$ for the KS4A3 and NS4A3 compositions, calculated at 0.5 mol% K_2O and Na_2O in the fluid, respectively, yields $D^{fluid/melt}_{K_2O}$ (KS4A3) = 0.13 and $D^{fluid/melt}_{Na_2O}$ (NS4A3) = 0.14. The actual values (from regression coefficients in Table 2) are 0.14 and 0.13, respectively. This correspondence between calculated and actual values lends further credence to the proposed solubility behavior of K_2O and Na_2O in these aqueous fluids.

For SiO_2, a smaller, but also positive, relationship to SiO_2 concentration in the fluid is observed (Table 2). Provided that silica in the aqueous fluid is dissolved via formation of depolymerized silicate complexes such as discussed above (e.g., Mysen, 1998; Zotov and Keppler, 2000), the behavior of dissolved silica may also be tied to the solution mechanisms of alkalis. As the systems become increasingly aluminous, an increasing fraction of the dissolved alkalis become associated with aluminate complexes. That in turn may reduce the availability of alkalis that could complex with the depolymerized silicate species in the fluid. As a result, the relationship between $D^{fluid/melt}_{SiO_2}$ and SiO_2 concentration in the fluid will depend on the Al_2O_3 content of the fluid.

4. CONCLUSIONS

1. Alkalis, silica, and to a lesser extent alumina dissolve incongruently in silicate-saturated fluids coexisting with silicate melts for peralkaline compositions in the systems Na_2O-Al_2O_3-SiO_2-H_2O and K_2O-Al_2O_3-SiO_2-H_2O in the 1- to 2-GPa pressure range at 1100°C. Alkalis show enrichment in the fluid, whereas silica is enriched in the coexisting melt. This effect diminishes with increasing pressure.

2. The fluid/melt partition coefficient for the individual oxides, $D^{fluid/melt}_{oxide}$, is a linear and positive function of the oxide concentration in the fluid. The partition coefficients for both alkalis and silica decreases with increasing alumina content of the fluid.

3. It is proposed that the alkalis dissolve in the fluid in at least two, and perhaps three, structurally different forms. These are alkali-OH complexes, some form of alkali aluminate complexes, and possibly alkali silicate complexes. As the alumina content increases, the aluminate complexes become more dominant and the values of $D^{fluid/melt}_{alkali}$ approach the values of $D^{fluid/melt}_{alumina}$, which is consistent with this solution model.

4. The solubility behavior of silica in the aqueous fluid is consistent with the formation of depolymerized silicate species. These silicate complexes probably are associated with alkalis. The negative correlation of $D^{fluid/melt}_{silica}$ with alumina probably reflects the multiple structural roles of alkalis in the fluid. A portion is associated with alumina to form aluminate complexes. As the alumina content increases, the abundance of aluminate may also increase thus lowering the concentration of alkali-associated silicate species in the fluid.

Acknowledgments—This research was conducted with partial support from NSF grants EAR-9901886 and REU-9619551.

Associate editor: M. S. Ghiorso

REFERENCES

Anderson G. M. and Burnham C. W. (1967) Reactions of quartz and corundum with aqueous chloride and hydroxide solutions at high temperatures and pressures. *Am. J. Sci.* **265,** 12–27.

Bebout G., Ryan J. G., and Leeman W. P. (1993) B-Be systematics in subduction-related metamorphic rocks; characterization of the subducted component. *Geochim. Cosmochim. Acta* **57,** 2227–2237.

Boyd F. R. and England J. L. (1960) Apparatus for phase equilibrium measurements at pressures up to 50 kilobars and temperatures up to 1750°C. *J. Geophys. Res.* **65,** 741–748.

Brenan J. M., Shaw H. F., Ryerson F. J., and Phinney D. L. (1995) Mineral-aqueous fluid partitioning of trace elements at 900° and 2.0 GPa: Constraints on the trace element geochemistry of mantle and deep crustal fluids. *Geochim. Cosmochim. Acta* **59,** 3331–3350.

Bureau H. and Keppler H. (1999) Complete miscibility between silicate melts and hydrous fluids in the upper mantle; experimental evidence and geochemical implications. *Earth Planet. Sci. Lett.* **165(2),** 187–196.

Burnham C. W. (1967) Hydrothermal fluids at the magmatic state. In *Geochemistry on Hydrothermal Ore Deposits* (ed. H. L. Barnes), pp. 34–67. Holt Rinehart and Winston.

Fowler M. B. (1984) Large-ion lithophile element mobility in the lower continental crust; mineralogy and geochemistry of the hornblende-granulite subfacies at Gruinard Bay and its relationships with amphibolite-facies and granulite-facies end members. In *Metamorphic Studies: Research in Progress* (ed. M. Brown), Vol. 141, p. 1076. Geological Society of London.

Frantz J. D. and Popp R. K. (1981) The ionization constants of aqueous $MgCl_2$ at elevated temperatures and pressures-a revision. *Geochim. Cosmochim. Acta* **45,** 2511–2512.

Fujii T., Mibe K., and Yasuda A. (1996) Composition of fluid coexisting with olivine and pyroxene at high pressure: The role of water on the differentiation of the mantle. In *Misasa Seminar on Evolutionary Processes of Earth and Planetary Materials*, pp. 37–38. Institute for the Study of the Earth's Interior, Okayama University, Misasa, Japan.

Haar L., Gallagher J. S., and Kell G. S. (1984) Steam tables. In *Thermodynamic and Transport Properties and Computer Programs for Vapor and Liquid States of Water in SI Units.* Hemisphere Publishing.

Kennedy G. C., Wasserburg G. J., Heard H. C., and Newton R. C. (1962) The upper three-phase region in the system SiO_2-H_2O. *Am. J. Sci.* **260,** 501–521.

Kushiro I. (1976) A new furnace assembly with a small temperature gradient in solid-media, high-pressure apparatus. *Carnegie Inst. Wash. Year Book* **75,** 832–833.

Manning C. E. (1994) The solubility of quartz in H_2O in the lower crust and upper mantle. *Geochim. Cosmochim. Acta* **58,** 4831–4839.

McInnes B. (1996) Fluid-peridotite interactions in mantle wedge xenoliths (abstract). *EOS Trans. Am. Geophys. Union* **77,** 282.

Morris J. D., Leeman W. P., and Tera F. (1990) The subducted component in island arc lavas: Constraints from Be isotopes and B-Be systematics. *Nature* **344,** 31–36.

Mysen B. O. (1987) Magmatic silicate melts: Relations between bulk composition, structure and properties. In *Magmatic Processes: Physiochemical Principles*, pp. 375–399. Special Publication 1. Geochemical Society

Mysen B. O. (1995) Experimental, in-situ, high-temperature studies of properties and structure of silicate melts relevant to magmatic temperatures. *Eur. J. Mineral.* **7,** 745–766.

Mysen B. O. (1998) Interaction between aqueous fluid and silicate melt in the pressure and temperature regime of the Earth's crust and upper mantle. *N. Nb. Mineral.* **172,** 227–244.

Mysen B. O. and Acton M. (1999) Water in H_2O-saturated magma-fluid systems: Solubility behavior in K_2O-Al_2O_3-SiO_2-H_2O to 2.0 GPa and 1300°C. *Geochim. Cosmochim. Acta* **63,** 3799–3816.

Mysen B. O. and Wheeler K. (2000a) Alkali aluminosilicate-saturated aqueous fluids in the Earth's upper mantle. *Geochim. Cosmochim. Acta* **64,** 4243–4256.

Mysen B. O. and Wheeler K. (2000b) Solubility behavior of water in haploandesitic melts at high pressure and high temperature. *Am. Mineral.* **85,** 1128–1142.

Nowak M. and Behrens H. (1997) An experimental investigation on diffusion of water in haplogranitic melts. *Contrib. Mineral. Petrol.* **126,** 365–376.

Osborn E. F. and Muan A. (1960a) Plate 4: The system Na_2O-Al_2O_3-SiO_2. In *Phase Equilibrium Diagrams for Ceramists.*American Ceramic Society.

Osborn E. F. and Muan A. (1960b) Plate 5: The system $K_2 \cdot O$-Al_2O_3-SiO_2. In *Phase Equilibrium Diagrams of Oxide Systems*. American Ceramic Society.

Paillat O., Elphick E. C., and Brown W. L. (1992) The solubility behavior of H_2O in $NaAlSi_3O_8$ melts: A re-examination of Ab-H_2O phase relationships and critical behavior at high pressure. *Contrib. Mineral. Petrol.* **112,** 490–500.

Pascal M. L. and Anderson G. M. (1989) Speciation of Al, Si, and K in supercritical solutions: Experimental study and interpretation. *Geochim. Cosmochim. Acta* **53,** 1843–1856.

Pitzer K. S. (1983) Dielectric constant of water at very high temperature and pressure. *Proc. Natl. Acad. Sci. USA* **80,** 4575–4576.

Plank T. and Langmuir C. H. (1993) Tracing trace elements from sediment input to volcanic output at subduction zones. *Nature* **362,** 739–743.

Quist S. A. and Marshall W. L. (1968) Electrical conductances of aqueous sodium chloride solutions from 0 to 700°C and pressures to 4,000 bars. *J. Phys. Chem.* **72,** 684–703.

Riter J. C. A. and Smith D. (1996) Xenolith constraints on the thermal history of the of the mantle beneath the Colorado Plateau. *Geology* **24,** 267–279.

Rollinson H. R. and Windley B. F. (1980) Selective elemental depletion during metamorphism of Archaean granulites, Scourie, NW Scotland. *Contrib. Mineral. Petrol.* **72,** 257–263.

Schneider M. E. and Eggler D. H. (1986) Fluids in equilibrium with peridotite minerals: Implications for mantle metasomatism. *Geochim. Cosmochim. Acta* **50,** 711–724.

Shen A. H. and Keppler H. (1997) Direct observation of complete miscibility in the albite-H_2O system. *Nature* **385,** 710–712.

Stalder R., Ulmer P., Thompson A. B., and Gunther D. (2000) Experimental approach to constrain second critical endpoints in fluid/silicate systems: Near-solidus fluids and melts in the system abite-H_2O. *Am. Mineral.* **85,** 68–77.

Stalder R., Ulmer P., Thompson A. B., and Gunther D. (2001) High pressure fluids in the system MgO-SiO_2-H_2O under upper mantle conditions. *Contrib. Mineral. Petrol.* **140,** 607–618.

Whitehouse M. J. (1989) Pb-isotopic evidence for U-Th-Pb behaviour in a prograde amphibolite to granulite facies transition from the Lewisian Complex of north-west Scotland; implications for Pb-Pb dating. *Geochim. Cosmochim. Acta* **53(3),** 717–724.

Zhang Y., Stolper E. M., and Wasserburg G. J. (1991) Diffusion of water in rhyolitic glasses. *Geochim. Cosmochim. Acta* **55(2),** 441–456.

Zhang Y.-G. and Frantz J. D. (2000) Enstatite–forsterite–water equilibria at elevated temperatures and pressures. *Am. Mineral.* **85,** 918–925.

Zotov N. and Keppler H. (2000) In situ Raman spectra of dissolved silica species in spectra of dissolved silica species in aqueous fluid to 900°C and 14 kbar. *Am. Mineral.* **85,** 600–603.